Exploring quantum quasicrystal patterns: A variational study

A. Mendoza-Coto,[1,*] R. Turcati,[1] V. Zampronio,[2] R. Díaz-Méndez,[3,4] T. Macrì,[2] and F. Cinti[5,6,7,†]

[1]*Departamento de Física, Universidade Federal de Santa Catarina, 88040-900 Florianópolis, Brazil*

[2]*Departamento de Fisica Teorica e Experimental, Universidade Federal do Rio Grande do Norte, 59078-970 Natal, Rio Grande do Norte, Brazil*

[3]*Ericsson Business Area Digital Services R&D, Ericsson Building 8, 164 40 Kista, Sweden*

[4]*Department of Physics, KTH Royal Institute of Technology, 106 91 Stockholm, Sweden*

[5]*Dipartimento di Fisica e Astronomia, Università di Firenze, I-50019, Sesto Fiorentino (Firenze), Italy*

[6]*INFN, Sezione di Firenze, I-50019, Sesto Fiorentino (Firenze), Italy*

[7]*Department of Physics, University of Johannesburg, P.O. Box 524, Auckland Park 2006, South Africa*

(Received 27 October 2021; revised 15 April 2022; accepted 15 April 2022; published 25 April 2022)

We study the emergence of quasicrystal configurations in the ground-state phase diagram of bosonic systems interacting through pair potentials of Lifshitz's type. By using a variational mean-field approach, we determine the relevant features of the corresponding potential interaction kind stabilizing such quasicrystalline states in two dimensions. Unlike their classical counterpart, in which the interplay between only two wave vectors determines the resulting symmetries of the solutions, the quantum picture relates in a more complex way to the instabilities of the excitation spectrum. Moreover, the quantum quasicrystal patterns are found to emerge as the ground state with no need of moderate thermal fluctuations. The study extends to the exploration of the excitation properties and the possible existence of superquasicrystals, i.e., supersolidlike quasicrystalline states in which the long-range nonperiodic density profile coexists with a nonzero superfluid fraction. Our calculations suggest that, in an intermediate region between the homogeneous superfluid and the normal quasicrystal phases, these exotic states indeed exist at zero temperature. Comparison with full numerical simulations provides a solid verification of the variational approach adopted in this paper.

DOI: 10.1103/PhysRevB.105.134521

I. INTRODUCTION

The exploration of patterns with peculiar symmetries such as stripe phases, smectic liquid crystals, cluster crystals, and quasicrystals is a leading research direction in many-body physics, unveiling a large amount of fascinating phenomena in soft matter [1,2], superconductivity [3,4], nonlinear optical systems [5–7], and long-range interacting systems in general [8–15]. In this context, quasicrystals are one of the most intriguing examples, as particles self-assemble in a long-range ordered pattern which is at the same time nonperiodic, thus being able to exhibit forbidden crystalline ordering such as 5-, 10-, and 12-fold rotational symmetry in two dimensions (2D).

For classical systems it has been shown that quasicrystalline phases may be originated thanks to the interplay between two specific length scales in the interaction potential of particle ensembles [16–19]. Many studies, based on mean-field and molecular dynamics approaches, have actually observed the stabilization of decagonal and dodecagonal cluster quasicrystals in soft macromolecular systems at finite temperatures by using this type of interactions [20–22]. While a recent theoretical work has surprisingly revealed the stability of those structures also at zero temperature for a particular case [23], the extent to which classical cluster quasicrystals can be stable in the absence of thermal fluctuations is a matter of debate.

On the other hand, quantum cluster quasicrystals have been studied by imposing external quasiperiodic potentials on bosonic systems, so creating quasicrystalline structures in, e.g., two-dimensional optical lattices [24,25]. Interestingly, the competition of interactions and quasiperiodicity generates a wide range of significant phases, such as supersolidity and Bose glasses [26–32].

In the absence of external potentials and for small temperatures, superfluidity was also investigated in a model relevant to the quantum cluster quasicrystal [33,34]. By using quantum Monte Carlo approaches, it was found that moderate quantum fluctuations make dodecagonal structures persist, leading to a small but finite local superfluid phase. Yet, by increasing fluctuations, a structural transition from quasicrystal to cluster triangular crystal takes place. In this scenario a natural question to ask is whether it is possible to produce cluster quasicrystal phases solely as a joined effect of quantum fluctuations and a properly designed interaction potential between particles. To our knowledge, the stabilization of self-assembled cluster quasicrystal states at zero temperature is a completely open question for generic interactions.

From the experimental standpoint, important steps have been taken to produce interactions with the necessary ingredients for the eventual stabilization of self-assembled quantum

*alejandro.mendoza@ufsc.br

†fabio.cinti@unifi.it

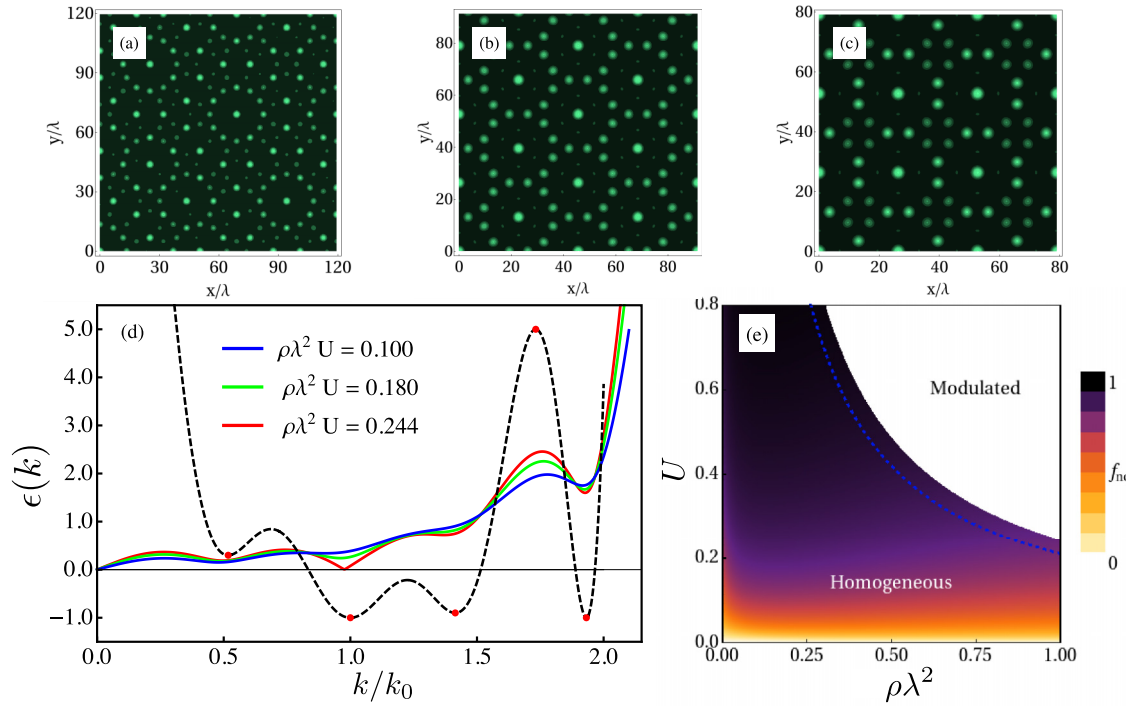

FIG. 1. (a)–(c) Real-space density for representative *Ansätze* resulting from the minimization of the energy of Eq. (1) for an ensemble of bosons interacting via the potential of Eq. (2). (a) Quasiperiodic pattern with 12-fold dodecagonal symmetry, (b) periodic pattern with sixfold hexagonal symmetry, and (c) periodic pattern with fourfold square symmetry. The parameters of the potential are as follows: $\hat{v}(0) = 20$, $\hat{v}(\sqrt{2}k_0) = 5$, $\hat{v}(\sqrt{3}k_0) = -0.9$, $\hat{v}(\sqrt{2-\sqrt{3}}k_0) = 0.3$, $\sigma = 1.2$, and $\rho\lambda^2 U = 1.0$ (see Sec. III). (d) Bogoliubov excitation spectrum $\epsilon(k)$ in units of $\hbar^2/(m\lambda^2)$ for different values of the product $\rho\lambda^2 U$ for the model considered in Sec. IV, selecting $\hat{v}(\sqrt{2-\sqrt{3}}k_0) = 0.3$ ($k_0 = 1$). The Fourier transform of the potential $\hat{v}(k)$ for the same parameters is also plotted (black dashed curve) for comparison with the energy excitation spectrum. (e) Phase diagram and noncondensed fraction f_{nc} computed self-consistently from Eq. (24). The blue dashed curve represents the phase boundary between the homogeneous and the dodecagonal cluster quasicrystal phase resulting from mean-field calculations. The color scale corresponds to the noncondensed fraction only within the region of stability of the homogeneous phase. Notice that Bogoliubov approximation holds when the noncondensed fraction $f_{nc} \ll 1$.

cluster quasicrystals. Current technology already allows us to produce effective oscillatory interactions with several length scales in multimode cavity QED. This kind of experimental setup give us the possibility of tuning the range of interactions providing means for the formation of various exotic phases as superfluid liquid-crystal-like states [35–37]. Another interesting direction in the production of effective interactions with various length scales was provided by Zhang *et al.* [38]. In that paper, the authors showed how a nonlocal sign-changing interaction between particles can be induced in a Bose-Einstein condensate (BEC) optically driven via a retroreflecting mirror. Additionally, they discussed how the sign of the underlying interaction potential can be controlled by additional optical elements and external fields. The kind of interaction induced by Zhang *et al.*'s [38] proposed setup is able to stabilize various nontrivial modulated phases, even nontrivial decorated lattices.

In this paper we address the problem of the stabilization of self-assembled quantum cluster quasicrystals through a variational mean-field (VMF) approach [39,40]. Our study allows us to identify the ingredients of the pair interaction potential needed for the stabilization of cluster quasicrystal states at zero temperature. As a result we present a systematic study of the mean-field phase diagrams for a class of bosonic models displaying quasicrystalline phases as well as other more common periodic and homogeneous superfluid phases. As an illustrative example, Fig. 1 depicts some stable density profiles for pattern configurations with 12-fold dodecagonal symmetry [Fig. 1(a)], sixfold hexagonal symmetry [Fig. 1(b)], and fourfold square symmetry [Fig. 1(c)] decorated with 12 smaller clusters. Here, we denote as triangular crystal phase (TCP) and square crystal phase (SqCP) any phase with the hexagonal and square symmetries, respectively, independent of the detailed structure of the unitary cell of the pattern. We highlight that the methodology developed in this paper is general and it can be used to design different types of potentials capable of stabilizing other modulated patterns. Additionally, we also probe the stability of the quasicrystal phase against generic perturbations of the pair interaction potential, showing that such a phase is not a result of a fine adjustment of the form of the potential.

Finally, we investigate the low-energy excitations in the homogeneous phase. The main result illustrated in Fig. 1(d) shows the Bogoliubov excitation spectrum for different values of $\rho\lambda^2 U$ properly tuning quasicrystal potentials, whereas Fig. 1(e) illustrates the phase diagram for the Bose-Einstein condensate fraction. The existence of superfluidity within quasicrystalline phases is also discussed. Our findings indicate the existence of supersolidlike quasicrystalline states in an intermediate phase between the homogeneous superfluid phase

and a normal cluster quasicrystal phase. Results obtained from our variational calculations are compared with its analogs obtained from the numerical integration of the Gross-Pitaevskii equation showing an excellent agreement.

The paper is organized as follows: Sec. II introduces the microscopic model specifying the methodology that was applied. Section III aims to present some important considerations by means of a first single-mode approximation. A characterization of a phase diagram varying the interaction strength and fixing the parametric potentials is proposed in Sec. IV. Furthermore, in Sec. V, we study the stability of the quantum quasicrystal phase against variations of the pair interaction potential. Section VI examines the chance to observe supersolid features in the system. Also within this section, we followed the Bogoliubov approach to discuss the excitation properties of the models considered. Finally, Sec. VII delivers some conclusions and remarks.

II. MODEL AND METHODOLOGY

We examine an ensemble of interacting bosons confined in 2D with mass m and position $\mathbf{q}_i$. The dynamics is described by the Hamiltonian

$$\hat{H} = -\frac{\hbar^2}{2m}\sum_i \nabla_i^2 + V_0 \sum_{i<j} v(|\mathbf{q}_i - \mathbf{q}_j|), \tag{1}$$

where V_0 is the interaction strength of the two-body potential $v(r)$. We introduce the energy scale of the problem as $\epsilon_0 = \hbar^2/(m\lambda^2)$, λ being the corresponding characteristic length. In doing so, we get the dimensionless term $U = V_0 m\lambda^2/\hbar^2$ which controls the zero-temperature physics at a fixed density $\rho\lambda^2$. Likewise, the dimensionless single-particle coordinate results as $\mathbf{r}_i = \mathbf{q}_i/\lambda$.

Our main goal is to study the possible stabilization of a 12-fold symmetric dodecagonal quasicrystal phase (QCP) at zero temperature. We choose nonlocal interaction potentials $v(r)$ of Lifshitz's type [21], whose Fourier transforms have the generic form

$$\hat{v}(k) = \exp(-k^2\sigma^2)\sum_{n=0}^{n_{\max}} D_n k^{2n}. \tag{2}$$

The free parameters D_n and σ can be tuned to guarantee a structure with several local minima at the desired wave vector; see Fig. 2. The high tunability of this class of potential allowed it to be established in the classical case that the stabilization of QCPs depends on the existence of a competition of different length scales [21,23,41,42].

Our study of the ground-state phase diagram is performed using the VMF approach [22,39,40,43–45]. Within the VMF approach the ground-state wave function, $\psi(\{\mathbf{x}\})$, where $\{\mathbf{x}\} = \{\mathbf{x}_1, \ldots, \mathbf{x}_N\}$, is first chosen as the product of identical single-particle wave functions

$$\psi(\{\mathbf{x}\}) = \prod_i \phi_0(\mathbf{x}_i). \tag{3}$$

Then, the normalized single-particle wave function $\phi_0(\mathbf{x})$ is written as a Fourier expansion using a specific set of modes

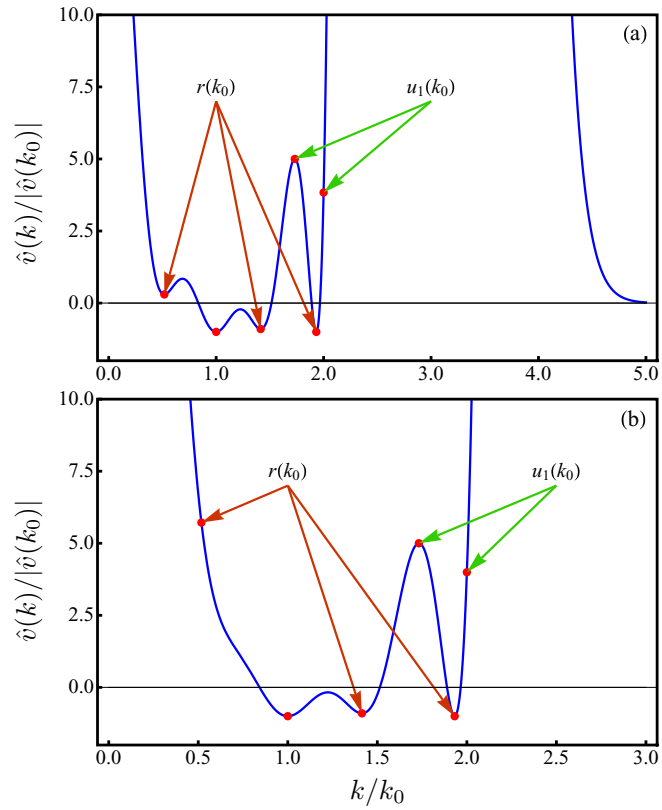

FIG. 2. Examples of Lifshitz's potentials able to stabilize the QCP as predicted from our variational development. The full form of $\hat{v}(k)$ in each case is obtained by imposing the following conditions: (a) $n_{\max} = 10$, $\hat{v}(0) = 20$, $\hat{v}(\sqrt{3-\sqrt{2}}k_0) = 0.3$, $\hat{v}(k_0) = -1$, $\hat{v}(\sqrt{2}k_0) = -0.9$, $\hat{v}(\sqrt{3}k_0) = 5$, and $\hat{v}(\sqrt{3+\sqrt{2}}k_0) = -1$ [in units of $|\hat{v}(k_0)|$] while $\sigma = 1.2$; and (b) $n_{\max} = 8$, $\hat{v}(0) = 70$, $\hat{v}(k_0) = -1$, $\hat{v}(\sqrt{2}k_0) = -0.9$, and $\hat{v}(\sqrt{3}k_0) = 5$ [in units of $|\hat{v}(k_0)|$] while $\sigma = 1$. In both panels the values of $\hat{v}(k)$ contributing to $r(k_0)$ and $u_1(k_0)$ are indicated. The latter functions are discussed throughout the main text.

$\{c_j, \mathbf{k}_j\}$ in the form [46,47]

$$\phi_0(\mathbf{x}) = \frac{c_0 + \sum_{j\neq 0} c_j \cos(\mathbf{k}_j \cdot \mathbf{x})/2}{\sqrt{A\left(c_0^2 + \frac{1}{4}\sum_{j\neq 0} c_j^2\right)}}, \tag{4}$$

where A is the area of the system. The set of Fourier modes considered in $\phi_0(\mathbf{x})$ defines the modulated pattern of the solution, as well as its symmetries.

In this paper we consider several *Ansätze* for $\phi_0(\mathbf{x})$ to minimize the Hamiltonian equation (1). More precisely, we take into account the homogeneous solution, a generic dodecagonal quasicrystal, and all possible periodic and symmetric patterns in two dimensions. For the special case of the homogeneous solution all c_j's vanish except for c_0. In the case of modulated patterns the number of independent Fourier amplitudes c_j can be significantly reduced by setting equal those Fourier amplitudes corresponding to wave vectors $\mathbf{k}_j$ equivalent by symmetry operations of the corresponding crystalline pattern. The set $\{\mathbf{k}_j\}$ is constructed considering all possible combinations of a predetermined finite number of wave vectors, taken as the basis of $\{\mathbf{k}_j\}$, which are specific for

TABLE I. Modulated patterns studied in this paper and the corresponding basis vectors used to generate the solutions $\phi(\mathbf{x})$. 12-QCP, 12-fold symmetric QCP.

Pattern	Basis vector $\mathbf{k}_{0,j}$	Index range
TCP	$k_0(\cos\frac{2\pi j}{6}, \sin\frac{2\pi j}{6})$	$j = 0, 1$
SqCP	$k_0(\cos\frac{2\pi j}{4}, \sin\frac{2\pi j}{4})$	$j = 0, 1$
Stripes	$k_0(1, 0)$	
12-QCP	$k_0(\cos\frac{2\pi j}{12}, \sin\frac{2\pi j}{12})$	$j = 0, 1, \ldots, 3$

each modulated solution. In this way, by fixing the number of vectors of the basis that can be combined to form $\{\mathbf{k}_j\}$, we can establish the order of the *Ansätze*. The *Ansätze* are summarized in Table I.

In all considered solutions the quantity k_0 represents the modulus of the wave vectors of the basis, which give us the scale of the modulation length of the respective pattern [48,49]. Fourier amplitudes c_j and k_0 are the variational parameters in the energy minimization process for each kind of solution.

The total energy per particle E/N of the model then reads

$$\frac{E}{N} = \langle\psi|\hat{T}_1|\psi\rangle + \frac{(N-1)}{2}\langle\psi|\hat{V}_{12}|\psi\rangle \tag{5}$$

$$= \frac{1}{4}\frac{\sum_{j\neq 0} c_j^2 k_j^2}{\left(1+\frac{1}{2}\sum_{j\neq 0} c_j^2\right)} + \rho\lambda^2 U \frac{\left(\hat{v}(0)b_0^2 + \sum_{j\neq 0}\hat{v}(k_j)b_j^2/2\right)}{2\left(1+\frac{1}{2}\sum_{j\neq 0} c_j^2\right)^2}, \tag{6}$$

where $\hat{T}_1 = -\frac{1}{2}\nabla_1^2$ is the usual single-particle kinetic energy operator while $\hat{V}_{12} = V(\mathbf{r}_1 - \mathbf{r}_2)$ is the two-body interaction operator in coordinate representation. In the above expression, we used the fact that $\mathbf{k}_j$ and $-\mathbf{k}_j$ have the same Fourier amplitude c_j. In addition, the coefficients b_j are defined as the Fourier amplitudes of $(\sum_{j=0} c_j \cos(\mathbf{k}_j\cdot\mathbf{x}))^2$; in this way the coefficients b_j can be written in terms of c_j using the relation $(\sum_{j=0} c_j \cos(\mathbf{k}_j\cdot\mathbf{x}))^2 = \sum_{j=0} b_j \cos(\mathbf{k}_j\cdot\mathbf{x})$, where the sum in both cases is considered over the whole set of vectors consistent with the symmetries of the considered modulated pattern. This energy is then compared with the energy of the homogeneous superfluid solution $\epsilon_{sf} = E_{sf}/N = \rho\lambda^2 U\hat{v}(0)/2$ [50].

III. SINGLE-MODE APPROXIMATION

We now identify the conditions to be satisfied by $\hat{v}(k)$ to stabilize the QCP over all other symmetric and periodic possible phases in two dimensions. We begin by performing a simple analysis of the necessary conditions to guarantee that the QCP has a lower energy than the sixfold symmetric TCP. The TCP configuration is selected as a benchmark for comparison with the QCP, since the triangular lattice corresponds to the optimal packing arrangement in two dimensions [29,51,52].

Within the single-mode approximation, i.e., considering solutions with Fourier modes corresponding only to the first shell of equivalent wave vectors, whose Fourier amplitudes are all equal to c_1, the energy per particle defined in Eq. (6) for the TCP is given by

$$\epsilon_t = \frac{1}{4}\frac{3c_1^2k_0^2}{\left(1+\frac{3}{2}c_1^2\right)} + \frac{\rho\lambda^2 U\hat{v}(0)}{2} + \rho\lambda^2 U\frac{\left(3c_1^2(2+c_1)^2\hat{v}(k_0) + u_1(k_0)c_1^4\right)}{4\left(1+\frac{1}{2}3c_1^2\right)^2}, \tag{7}$$

where $u_1(k) = (3/4\hat{v}(2k) + 3\hat{v}(\sqrt{3}k))$. Modulated phases can usually be stabilized if the absolute minimum of $\hat{v}(k)$ is lower than zero and it simultaneously occurs at some finite wave vector modulus k_m [43]. In general, the variational treatment of the modulation wave vector k_0 produces nontrivial results which depend on the detailed form of $\hat{v}(k)$, even within the single-mode approximation. In principle one might expect k_0 to be close to k_m if the minimum of $\hat{v}(k)$ at k_m is strong enough and we are close to the boundary between the homogeneous and the modulated phases, where we expect $c_1 \ll 1$. Nevertheless, establishing rigorous conditions for $\hat{v}(k)$, under which the single mode is in fact a good approximation, is a very difficult task.

With the aim of identifying general ingredients, independent of the actual form of our $\hat{v}(k)$, we begin by considering a single-mode analysis in which k_0 is fixed to k_m. In a subsequent step, we will perform a full variational analysis for specific cases of $\hat{v}(k)$ considering solutions with many modes to verify to what extent the conclusions about the stability of the QCP, from this simplified study, remain valid in the general case.

Without loss of generality we take advantage of the fact that, in the appropriate units, the position of the main minimum of $\hat{v}(k)$ can be located at $k_0 = 1$, and its value can be set to $\hat{v}(k_0) = -1$.

The other relevant phase in our simplified single-mode analysis corresponds to the dodecagonal QCP. Considering Eq. (6) and the proposed *Ansätze* for this phase, it is straightforward to conclude that the energy per particle for the QCP is given by

$$\epsilon_{\rm QCP} = \frac{1}{4}\frac{6c_1^2k_0^2}{\left(1+\frac{6}{2}c_1^2\right)} + \frac{\rho\lambda^2 U\hat{v}(0)}{2} + \rho\lambda^2 U\frac{\left(6c_1^2(2+c_1)^2\hat{v}(k_0) + u_2(k_0)c_1^4\right)}{4\left(1+\frac{1}{2}6c_1^2\right)^2}, \tag{8}$$

where $u_2(k) = 2u_1(k) + r(k)$ and $r(k) = 6(\hat{v}(\sqrt{2}k) + \hat{v}(\sqrt{2-\sqrt{3}}k) + \hat{v}(\sqrt{2+\sqrt{3}}k))$.

It can be observed that the influence of $\hat{v}(k)$ on the energy per particle of the two relevant phases is encoded in two independent parameters, $r(k_0)$ and $u_1(k_0)$. Now we can compare the energy per particle of the TCP and QCP after minimizing with respect to the variable c_1, fixing the value of $u_1(k_0)$ and varying the parameters $\rho\lambda^2 U$ and $r(k_0)$. We observe in Fig. 3 that, for large enough $\rho\lambda^2 U$ values, the QCP becomes stable if $r(k_0)$ is low enough. This result confirms our initial expectation that if we decrease the value of the quartic coefficient for the QCP [$u_2(k_0)$], while maintaining $u_1(k_0)$ at

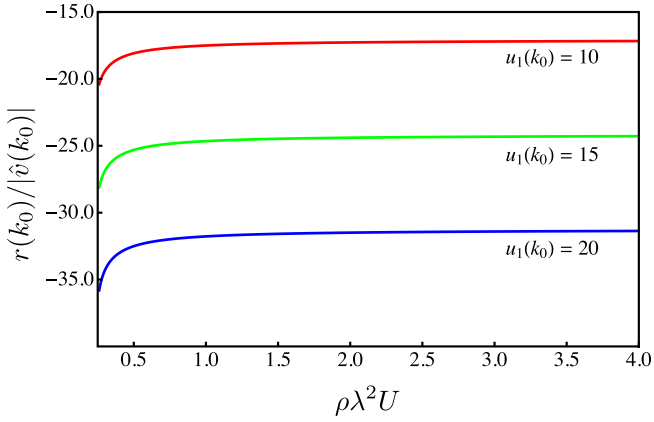

FIG. 3. Boundary between the dodecagonal cluster quasicrystal phase and the triangular cluster crystal in the $r(k_0)$-$\rho\lambda^2 U$ plane for $u_1(k_0) = 10$, 15, and 20, in units of $|\hat{v}(k_0)|$. For each case the region below the curve corresponds to those cases in which the dodecagonal solution has lower energy than the triangular lattice.

a moderate to high value, the relative stability of the QCP is increased.

We can infer now that a sufficient condition for $\hat{v}(k)$ to stabilize the QCP will be to have low enough local minima, at $\sqrt{3-\sqrt{2}}k_0$, k_0, $\sqrt{2}k_0$, and $\sqrt{3+\sqrt{2}}k_0$, to decrease $r(k_0)$ and to have local maxima or at least moderate values, at $\sqrt{3}k_0$ and $2k_0$, in order to obtain "high" values of $u_1(k_0)$. For future reference we will denote the values of $\hat{v}(k)$ at these particular points as characteristic values of the pair interaction potential. Physically, this set of wave vectors is relevant in our analysis because they correspond to the second-order harmonic of the Fourier representation of the dodecagonal solution. Additionally, it is observed that, given the form of the Lifshitz potential, a high value of $\hat{v}(2k_0)$ is already guaranteed by the sequence of maxima and minima of the potential. It can be concluded that a potential with 11 D_n independent coefficients ($n_{\max} = 10$) is needed in order to build a $\hat{v}(k)$ for which all the characteristic values can be tuned to produce a potential with the desired features.

This discussion raises the question of what the actual minimum value of $n_{\max}$ to maintain the stability of the QCP would be once we abandon the single-mode approximation. We have studied this problem numerically by means of a many-mode variational treatment of Eq. (6), considering the 12-fold QCP and all other periodic and rotationally symmetric solutions in two dimensions. This constraint rules out the possibility of stretched periodic lattices in our analysis. Our results indicate that the secondary minimum at $\sqrt{2-\sqrt{3}}k_0$ is in fact not a necessary ingredient beyond the single-mode analysis. To the best of our knowledge, the simplest Lifshitz's model stabilizing the QCP is the one with $n_{\max} = 8$; however, we cannot rule out the possibility of stabilization of the QCP through a two-body interaction with simpler structures than those we are considering now.

IV. PHASE DIAGRAM CHARACTERIZATION

Before presenting the results of the numerical study, we provide some details about the construction of the solutions

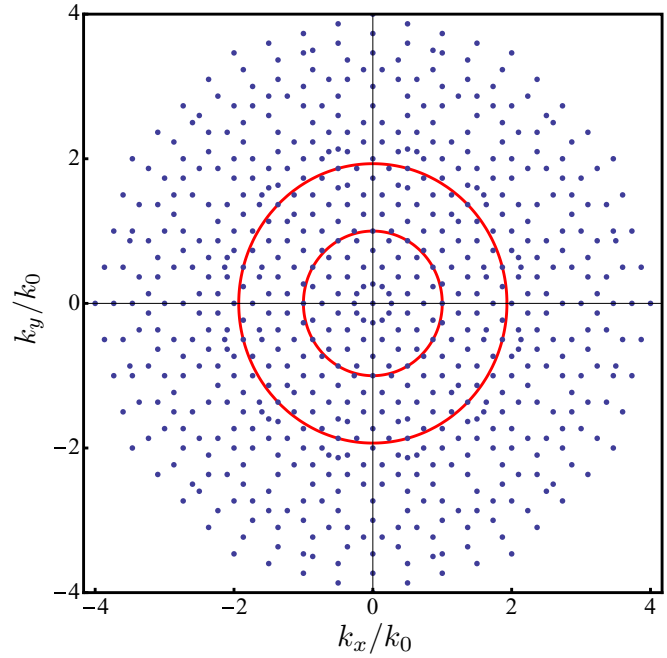

FIG. 4. Wave vectors considered in the construction of the fourth-order dodecagonal solution in units of the basis wave vector k_0. Red circles show the two degenerate minima of the Fourier transform of the potential $\hat{v}(k)$.

in the case of the many-mode numerical analysis. Due to the aperiodic nature of the dodecagonal pattern, the set of wave vectors corresponding to the Fourier mode expansion of this solution rapidly increase when even a moderate number of possible combinations of wave vectors of the basis is considered. In the numerical analysis we consider a fourth-order *Ansatz* for the QCP solution, which means that all vectors resulting from the combinations of four vectors of the basis and the null vector will be considered. The resulting set of wave vectors considered in the construction of this solution is shown in Fig. 4. This selection implies that the QCP solution has 37 independent Fourier amplitudes [c's in Eq. (4)], which are then considered as variational parameters, jointly with the scale of the main wave vector k_0. The number of variational Fourier amplitudes for each periodic solution is given by the following: 34 for the TCP, 33 for the SqCP, and 10 for the stripes solution.

We will study the mean-field phase diagram of the kind of Lifshitz's models previously described using the canonical ensemble. Since we are exclusively interested in the ground-state properties, the phase diagrams will be calculated after an energy minimization process considering the set of possible solutions described in Table I. We further simplify our analysis considering that only pure phases are possible. Consequently, coexistence regions are not presented in our simplified phase diagrams even when all the transitions obtained are first order. This is a common simplification when we are working with quantum gas models in which coexistence regions are expected to be narrow.

In Fig. 5(a) the results of the minimization are shown for a class of potentials given by the following set of $n_{\max} = 10$ characteristic values: $\hat{v}(0) = 20$, $\hat{v}(\sqrt{3}k_0) = -0.9$,

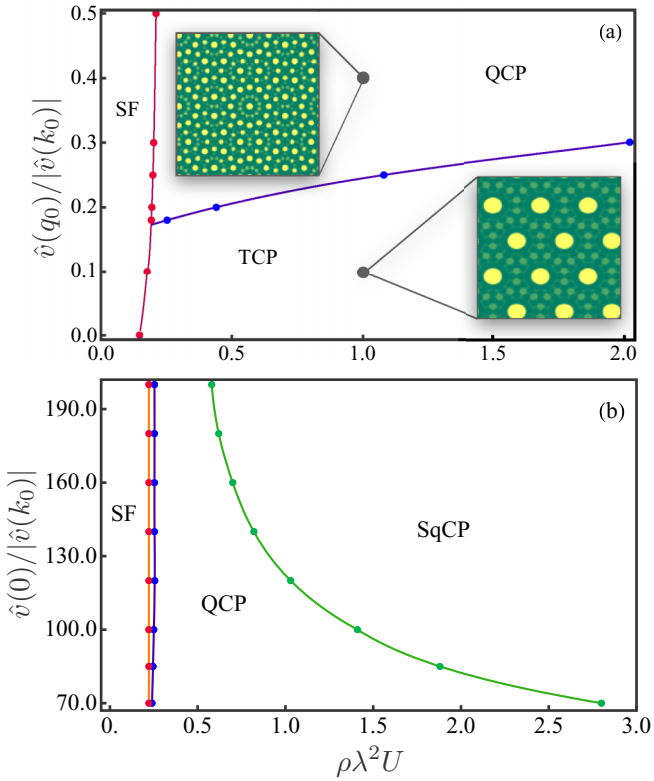

FIG. 5. Ground-state phase diagrams in the $\rho\lambda^2 U$ vs $\hat{v}(q_0)$ plane for the two families of potentials given by Eq. (2), using $n_{\max} = 10$ (a) and $n_{\max} = 8$ (b). The parameters of the potential are as follows. (a) $\sigma = 1.2$, $q_0 = \sqrt{2-\sqrt{3}}k_0$, while being subjected to the constraints $\hat{v}(0) = 20$, $\hat{v}(\sqrt{2}k_0) = -0.9$, $\hat{v}(\sqrt{3}k_0) = 5$, $\hat{v}(\sqrt{3+\sqrt{2}}k_0) = -1$, in units of $|\hat{v}(k_0)|$. The insets display two configurations referring to the TCP [$\rho\lambda^2 U = 1$ $\hat{v}(q_0)/|\hat{v}(k_0)| = 0.1$] and QCP [$\rho\lambda^2 U = 1$ $\hat{v}(q_0)/|\hat{v}(k_0)| = 0.4$], respectively. Configurations have been obtained solving numerically the Gross-Pitaevskii equation (see Sec. VI). (b) $\sigma = 1$, $q_0 = 0$, while being subjected to the constraints $\hat{v}(\sqrt{2}k_0) = -0.9$, $\hat{v}(\sqrt{3}k_0) = 5.0$, in units of $|\hat{v}(k_0)|$.

$\hat{v}(\sqrt{2}k_0) = 5$, and $\sigma = 1.2$; $\hat{v}(\sqrt{2-\sqrt{3}}k_0) \in [0, 1/2]$ is left as a free parameter.

It can be observed that, for low values of $\hat{v}(\sqrt{2-\sqrt{3}}k_0)$, as the product $\rho\lambda^2 U$ is increased there is a transition from the homogenous superfluid (SF) phase to the TCP. This means that for such pair interaction potentials the TCP is favored over the QCP [see Fig. 5(a)]. However, as this quantity is increased up to some critical value of $\hat{v}(\sqrt{2-\sqrt{3}}k_0)$, a region of stability of the QCP at intermediate values of $\rho\lambda^2 U$ is developed.

Interestingly enough, the previous results show that large values of $\hat{v}(\sqrt{2-\sqrt{3}}k_0)$ do not eliminate the stability of the QCP. This fact suggests that a low value of $\hat{v}(\sqrt{2+\sqrt{3}}k_0)$ is not actually a necessary condition for the stability of the QCP beyond the single-mode approximation. It implies that we can further reduce the order of the polynomial considered in the definition of Eq. (2). This is related to the fact that the distribution of modes forming the QCP solution is much denser than the one we have for a periodic lattice. Consequently, there is a greater number of modes with wave vectors close to the optimal ones, which increase significantly the stability of the solution.

Considering the discussion above, we analyze now the case of a simpler model with $n_{\max} = 8$. As in the previous case all free parameters D_n will be determined from the characteristic values of the potential: $\hat{v}(\sqrt{2}k_0) = -0.9$, $\hat{v}(\sqrt{3}k_0) = 5.0$, and $\sigma = 1$, while $\hat{v}(0) \in [70, 120]$ was taken as the free parameter. The results of the minimization process are shown in Fig. 5(b).

As in Fig. 5(a), the QCP corresponds to the most stable phase over a wide $\rho\lambda^2 U$ region. However, it can be noticed that there is not a direct transition from the homogeneous SF phase to the QCP. Instead, there is a narrow region between these two phases in which the TCP is the most stable phase. Additionally, for large enough values of $\rho\lambda^2 U$, there is always a transition to the SqCP.

V. STABILITY OF THE QCP

To analyze the stability of the QCP with respect to small perturbations of the form of the potential, we consider the energy per particle given in Eq. (6) for arbitrary *Ansätze* of the ground-state wave function, which can be recast as

$$\frac{E}{N} = \langle\phi|\,\hat{T}\,|\phi\rangle + \frac{u}{2}A\langle\phi^2|v(x)|\phi^2\rangle, \tag{9}$$

where the brackets in the above equation are given by $\langle\phi|\hat{T}|\phi\rangle = -1/2\int d\mathbf{x}\phi(\mathbf{x})\nabla^2\phi(\mathbf{x})$ and $\langle\phi^2|v(x)|\phi^2\rangle = \int d\mathbf{x}d\mathbf{x}'\phi^2(\mathbf{x})v(\mathbf{x}-\mathbf{x}')\phi^2(\mathbf{x}')$, respectively. We can notice that the first and second terms on the right-hand side of Eq. (9) correspond to the average kinetic and potential energy per particle, while the parameter u is shorthand for the product $\rho\lambda^2 U$.

Let us assume that for a pair interaction potential $\hat{v}_0(k)$, the QCP is the lowest energy state per particle in the interval $u \in (u_1, u_2)$. As a consequence, in this interval, $\epsilon_q(u) < \epsilon_2(u)$, where $\epsilon_q(u)$ and $\epsilon_2(u)$ represent the energy per particle of the QCP and that of a secondary phase, respectively.

In the presence of a small perturbation $\delta\hat{v}(k)$ of the pair interaction potential, the energy per particle of the QCP yields

$$\epsilon_q = \epsilon_{q,0}(\{c_j\}, k_0) + u\frac{\left(\delta\hat{v}(0)b_0^2 + \sum_{j\neq 0}\delta\hat{v}(k_j)b_j^2/2\right)}{2\left(1+\frac{1}{2}\sum_{j\neq 0}c_j^2\right)^2}, \tag{10}$$

where $\epsilon_{q,0}(\{c_j\}, k_0)$ stands for the energy function of the QCP in the absence of perturbation, $\{c_j\}$ is the set of Fourier coefficients of the QCP solution of the full problem, and k_0 is the corresponding modulation wave vector. We then expand the energy per particle ϵ_q of Eq. (10) up to first order in $\delta\hat{v}(k)$, considering first that the $\{c_j\}$ and k_0 corresponding to the optimal solution of the perturbed problem can be also expanded in powers of $\delta\hat{v}(k)$. After some algebra we obtain

$$\epsilon_q = \epsilon_{q,0}(\{c_{j,0}\}, k_{0,0}) + u\frac{\left(\delta\hat{v}(0)b_{0,0}^2 + \sum_{j\neq 0}\delta\hat{v}(k_{j,0})b_{j,0}^2/2\right)}{2\left(1+\frac{1}{2}\sum_{j\neq 0}c_{j,0}^2\right)^2}, \tag{11}$$

where $\{c_{j,0}\}$ and $k_{0,0}$ represent the optimal Fourier amplitudes and modulation wave vector of the unperturbed problem,

respectively. Here, we have already taken into account that $\partial_{c_j}\epsilon_{q,0}(\{c_{j,0}\}, k_{0,0}) = 0$ and $\partial_{k_0}\epsilon_{q,0}(\{c_{j,0}\}, k_{0,0}) = 0$, as well as the fact that the lowest-order corrections to c_j and k_0, corresponding to the optimal solution of the perturbed problem, are linear in $\delta\hat{v}(k)$.

The unperturbed problem could admit, in principle, more than one solution of the same kind. Considering that our analysis relies on the stability of the solutions of the original problem against perturbations, a required condition is the existence of a finite energy gap between the energy corresponding to the optimal solution and those corresponding to any other solutions of the same kind. If such a gap exists, then it is always possible to use perturbation theory around the optimal solution of the unperturbed problem for small enough $\delta\hat{v}(k)$. The result obtained for the energy correction of the optimal QCP solution is also valid for other phases, since at any point we have taken advantage of the particular form of the QCP solution. The corrected energy per particle as a function of the parameter u will be then

$$\epsilon_q(u) = \epsilon_q^0(u) + \frac{u}{2}A\langle\phi_{q,0}^2|\delta v(x)|\phi_{q,0}^2\rangle,$$
$$\epsilon_2(u) = \epsilon_2^0(u) + \frac{u}{2}A\langle\phi_{2,0}^2|\delta v(x)|\phi_{2,0}^2\rangle. \tag{12}$$

Now it is possible to compute, up to first order in $\delta v(x)$, the solution of the equation $\epsilon_q(u) = \epsilon_2(u)$, which gives us the location of the phase boundary after perturbing the pair interaction potential. Considering that at $u = u_1$, $\epsilon_q^0(u_1) = \epsilon_2^0(u_1)$ holds, we conclude that up to first order in $\delta v(x)$ the correction to the phase boundary position reads

$$\delta u = \frac{u_1}{2}\frac{\left(A\langle\phi_{2,0}^2|\delta v(x)|\phi_{2,0}^2\rangle - A\langle\phi_{q,0}^2|\delta v(x)|\phi_{q,0}^2\rangle\right)}{\left(\partial_u\epsilon_q^0(u_1) - \partial_u\epsilon_2^0(u_1)\right)}. \tag{13}$$

This result shows that, if for a specific $\hat{v}(k)$ the QCP corresponds to the ground state of the system in a certain finite region of the parameter $\rho\lambda^2 U$, then arbitrary small enough perturbations of $\hat{v}(k)$ will not destroy the stability of the QCP.

VI. SUPERSOLIDITY WITHIN THE QCP

The supersolid phase is a state of matter that breaks both continuous translational and global U(1) symmetries, exhibiting simultaneously a crystalline order and an off-diagonal long-range order [29,53]. Many efforts from the theoretical perspective [28,29,53–58] as well as several low-temperature experiments with dipolar quantum gases [59–64] have been realized in recent years to understand the properties and the existence of these density-modulated superfluid systems.

In order to analyze whether a supersolidlike phase could be stabilized within the QCP, we consider two parameters quantifying both superfluid and quasicrystalline order. We employ Leggett's criterion [55,65], which allows us to compute an upper bound for the superfluid fraction as

$$f_s = \mathrm{Min}_\theta\left[\int\frac{d^2\mathbf{x}}{A}\frac{1}{\int_0^L\frac{dx}{L}\rho(x',y')^{-1}}\right], \tag{14}$$

where the function $\rho(x,y) = A|\phi_0(x,y)|^2$ and A and L stand for the area and linear dimension of the system, respectively. In this equation, we should take the minimum with respect to all possible directions defined by the angle θ, taking $x' = x\cos\theta - y\sin\theta$ and $y' = x\sin\theta + y\cos\theta$. Instead of proceeding directly with the numerical calculation of f_s it is convenient first to discuss some mathematical properties of the quantity defined in Eq. (14), which can lead to a simplification of the numerical evaluation of f_s.

Let us begin analyzing the quantity $\int dx/L\rho^{-1}(x',y')$ in the limit $L\to\infty$, which is in principle a function of y and θ. If $\phi_0(\mathbf{x})$ is a periodic or quasiperiodic function, then $\rho^{-1}(\mathbf{x})$ will have the same symmetry properties of $\phi_0(\mathbf{x})$, and consequently the same full set of Fourier modes can be used in general to expand $\rho(\mathbf{x})$ and $\rho^{-1}(\mathbf{x})$.

Therefore, without loss of generality, for configurations for which $\int\frac{d^2\mathbf{x}}{L^2}\rho(\mathbf{x})^{-1}$ is finite, $\rho^{-1}(\mathbf{x})$ can be written as

$$\rho^{-1}(x',y') = d_0 + \sum_{i\neq 0} d_i\cos[(k_{ix}\cos(\theta) + k_{iy}\sin(\theta))x + (k_{iy}\cos(\theta) - k_{ix}\sin(\theta))y], \tag{15}$$

where $\{k_{ix}, k_{iy}\}$ represent the Cartesian components of $\mathbf{k}_i$ and the d_i's represent the Fourier amplitudes of $\rho^{-1}(x,y)$, defined in the usual way. Proceeding with the formal integration along the x variable, and taking $L\to\infty$, we find

$$\int_0^L\frac{dx}{L}\rho^{-1}(x',y') = d_0 + \sum_{i\neq 0} d_i\cos[(k_{iy}\cos(\theta) - k_{ix}\sin(\theta))y] \times\delta(k_{ix}\cos(\theta) + k_{iy}\sin(\theta), 0), \tag{16}$$

where $\delta(a,b)$ stands for the Kronecker delta function. This result implies that, unless θ is selected to be one of the possible discrete values for which $k_{ix}\cos(\theta) + k_{iy}\sin(\theta) = 0$, the result of the integration is a constant equal to d_0.

Now we can take advantage of the Schwarz inequality, which allows us to conclude directly that

$$\int\frac{dy}{L}\frac{1}{\int\frac{dx}{L}\rho^{-1}(x',y')} \geqslant \frac{1}{\int\frac{dy}{L}\int\frac{dx}{L}\rho^{-1}(x',y')}. \tag{17}$$

Considering then the form of Eq. (16), or even Eq. (15), it is straightforward to conclude that

$$\int\frac{dy}{L}\frac{1}{\int\frac{dx}{L}\rho^{-1}(x',y')} \geqslant \frac{1}{d_0}. \tag{18}$$

Since this inequality holds for all θ and only becomes an identity when θ corresponds to one of those values which makes zero the oscillatory dependence in y of the right-hand side of Eq. (16), we can conclude that

$$\mathrm{Min}_\theta\left[\int\frac{dy}{L}\frac{1}{\int\frac{dx}{L}\rho^{-1}(x',y')}\right] = \frac{1}{d_0}. \tag{19}$$

This means that the superfluid fraction given by Eq. (14) is $f_s = \frac{1}{d_0}$. As a consequence, from now on we will adopt this expression as our definition of the superfluid fraction.

We observed that for large enough $\rho\lambda^2 U$, numerical issues in the variational minimization process eventually produce spurious solutions with nodes, leading to a vanishing superfluid fraction. This effect is not present in the full numerical solution of the Gross-Pitaevskii equation [50] (see the following discussion).

The crystalline order of the modulated patterns can be characterized by using the so-called density contrast, defined as [61–63]

$$C = \frac{\max[\rho(\mathbf{x})] - \min[\rho(\mathbf{x})]}{\max[\rho(\mathbf{x})] + \min[\rho(\mathbf{x})]}. \tag{20}$$

For states without density modulations, the parameter C vanishes. On the other hand, for strongly density-modulated states, C is close to unity.

In the case of quasicrystalline patterns, the determination of the contrast has the inherent complication related to the fact that the maximum and minimum of the profile density are not well-defined single values. Instead, in that case, there is a distribution of local maxima and minima over the system, and in general, the calculus of the absolute minimum and maximum of the profile density is a difficult task.

In our case, given the form of the *Ansätze* for the single-particle wave function, the absolute maximum is located at the origin of the coordinate system. However, the determination of the absolute minimum of the density profile is far from trivial. Because of this, we adopt the simplifying criterion of taking the minimum of the density profile as that of the local minimum closest to the absolute maximum. Such a value can be determined numerically by a simple minimization procedure of $\rho(\mathbf{x})$. In Fig. 6 the behavior of both the superfluid fraction f_s and the density contrast C is presented for the model given by Eq. (2) with $n_{\max} = 10$, considering two different inputs for the characteristic value $\hat{v}(\sqrt{3-\sqrt{2}}k_0)$. The obtained results confirm in both cases a sequence of superfluid and supersolidlike QCPs as $\rho\lambda^2 U$ is increased from low values. A discontinuous phase transition is clearly observed from the homogeneous SF phase to the supersolidlike QCP at $\rho\lambda^2 U \sim 0.23$. As a test for the validity of the mean-field (MF) variational observations presented in Fig. 6(a) we have computed f_s and C for this case from numerical simulations of the Gross-Pitaevskii equation (GPE). We observe that the first-order transition is slightly shifted with respect to the variational value. After this transition region the agreement obtained between analytical and numerical simulation results is excellent giving in this way a strong validation of our variational study.

For the numerical simulations, we considered the solution of the GPE in imaginary time in order to project the ground state from a given *Ansatz*. Written with the aforementioned dimensionless quantities, the imaginary-time GPE is

$$\frac{\partial\phi(\mathbf{r},\tau)}{\partial\tau} = \left[\frac{1}{2}\nabla^2 - N\int d\mathbf{r}' v(\mathbf{r}-\mathbf{r}')|\phi(\mathbf{r}',\tau)|^2\right]\phi(\mathbf{r},\tau), \tag{21}$$

where ϕ is normalized to unity. The convolution integral related to the nonlocal interaction is carried out in Fourier space:

$$\mathcal{F}\left[\int d\mathbf{r}' v(\mathbf{r}-\mathbf{r}')|\phi(\mathbf{r}',\tau)|^2\right] = \hat{v}(\mathbf{k}) \times \hat{n}(\mathbf{k},\tau). \tag{22}$$

The Fourier transform of the interaction potential $\hat{v}(\mathbf{k})$is given in Eq. (2), and we implement numerical fast Fourier transforms (FFTs) of the density $\hat{n} = \mathcal{F}[|\phi|^2]$. After computing Eq. (22) we apply an inverse FFT to obtain the convolution in

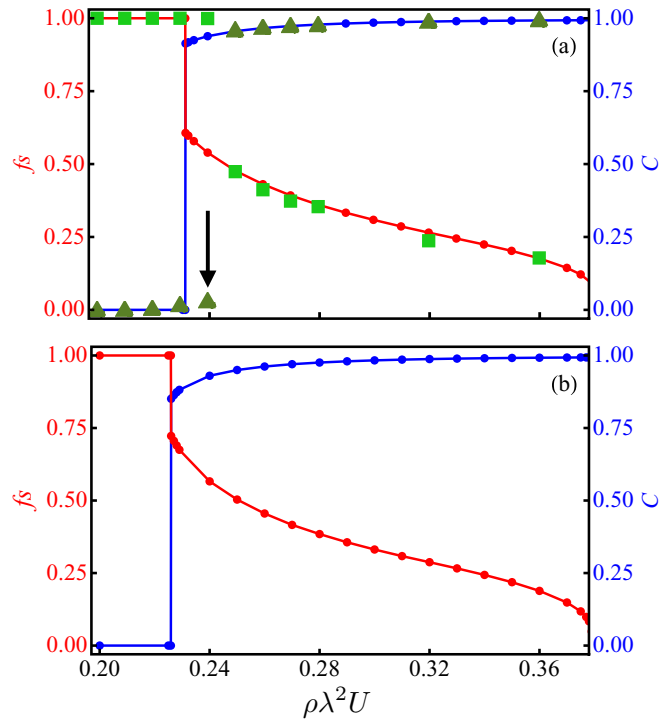

FIG. 6. Density contrast and superfluid fraction as a function of $\rho\lambda^2 U$, setting $\hat{v}(\sqrt{3-\sqrt{2}}k_0) = 5$ (a) and $\hat{v}(\sqrt{3-\sqrt{2}}k_0) = 10$ (b). The rest of the characteristic parameters of the potential are the same as in Fig. 2(a). Two different phases can be distinguished: the superfluid phase in which $C = 0$ and $f_s = 1$ and the supersolidlike QCP in which $C > 0$ and $0 < f_s < 1$. In (a), squares and triangles in green correspond to the superfluid fraction and to the density contrast computed from the direct numerical solution of the Gross-Pitaevskii equation, respectively. Additionally, the black arrow marks the transition from the superfluid to the supersolidlike QCP also obtained from Gross-Pitaevskii simulations.

Eq. (21). In all simulations the initial *Ansätze* were Gaussians centered at the middle of the simulation box. The numerical solution of the GPE using adaptive Runge-Kutta algorithms and the FFTs were implemented in XMDS2 software [66]. The sizes of the simulation box were chosen to fit the *Ansatz* that minimizes the VMF energy for a given set of parameters.

Now we focus on the excitation properties of the homogeneous phase in the presence of potentials stabilizing the QCP. Within the Bogoliubov theory, the low-energy excitation spectrum within the superfluid phase can be written as [50,67]

$$\epsilon(k,\rho\lambda^2 U) = \sqrt{\frac{k^2}{2}\left(\frac{k^2}{2} + 2\rho\lambda^2 U\hat{v}(k)\right)}. \tag{23}$$

In Fig. 1(d) the excitation spectrum for several values of $\rho\lambda^2 U$ is shown. For comparison, a plot of the $\hat{v}(k)$ used in these calculations is also included.

The sequence of local minima in $\epsilon(k)$, for intermediate values of $\rho\lambda^2 U$, closely reproduces the sequence of local minima in $\hat{v}(k)$. At large enough values of $\rho\lambda^2 U$, the excitation spectrum develops several roton minima corresponding to the various minima of $\hat{v}(k)$. Due to the competition between the kinetic energy term and the pair interaction potential in $\epsilon(k)$,

the dominant roton minimum position changes from a value close to $\sqrt{2-\sqrt{3}}k_0$ to a value close to k_0 as the density increases, which leads to the destabilization of the homogeneous phase at a wave vector which is essentially k_0. As expected, since the homogeneous-to-modulated transition is first order, we already know that the limit of stability of the homogeneous phase should be located at values of $\rho\lambda^2 U$ higher than those corresponding to the boundary of the homogeneous phase previously determined (see Fig. 1).

Another quantity of interest which is accessible from the Bogoliubov theory is the so-called normalized condensate depletion f_{nc} characterizing the noncondensed fraction of the system

$$f_{nc} = \frac{1}{\rho}\int \frac{d^2k}{(2\pi)^2}\frac{1}{2}\left[\frac{\frac{k^2}{2}+\rho_0 U\hat{v}(k)}{\epsilon(k,\rho_0 U)}-1\right], \qquad (24)$$

where ρ_0 represent the particle density of the condensate [68,69]. The noncondensed fraction can be determined self-consistently from the relation $\rho_0 = \rho(1-f_{nc})$, a condition that guarantees the proper normalization of f_{nc}, i.e., $0 \leqslant f_{nc} \leqslant 1$.

In Fig. 1(e), a phase diagram of $\rho\lambda^2$ versus U is presented describing the Bose-Einstein condensation in the homogeneous state for the model given by Eq. (2), using the same set of characteristic values considered in Fig. 2(a). A crossover of f_{nc} from low to high values can be observed as U is increased. We have highlighted with a green curve the boundary of the region of the high noncondensed fraction ($f_{nc} > 0.9$). This boundary is not monotonic, revealing a nontrivial interplay between the density and the potential strength.

VII. CONCLUSIONS

In this paper we analyzed under which conditions a cluster quasicrystal phase is self-stabilized in a 2D system of interacting bosons at zero temperature. We used the VMF approach firstly to identify the necessary ingredients to stabilize a dodecagonal quasicrystal modulated pattern in a model interacting through a Lifshitz-type potential and, in a second stage, to systematically study the complete phase diagram of these models varying the form of the pairwise potential. Our numerical studies considered several *Ansätze* for the modulated phases. We determined that, depending on the form of the pair interaction potential, the cluster QCP can be stabilized in a wide $\rho\lambda^2 U$ interval, ranging from the boundary of the homogeneous phase to the classical regime at large $\rho\lambda^2 U$ values.

This scenario suggests the possibility of the existence of a supersolidlike QCP and a classical QCP in which the superfluid fraction is finite and zero, respectively. The stability of this QCP against small variations of $\hat{v}(k)$ was also confirmed. Additionally, we showed that, once the QCP is stable for a given $\hat{v}(k)$ in a certain region of the parameter $\rho\lambda^2 U$, small enough variations $\delta\hat{v}(k)$ in the pair interaction potential smoothly change the $\rho\lambda^2 U$ region of stability of the QCP.

The excitation properties within the homogeneous phase for models stabilizing the QCP were studied by monitoring the Bogoliubov spectrum for a wide interval of $\rho\lambda^2 U$. In general, a structure of local minima was observed that closely follows the one observed for the pair interaction potential. For $\rho\lambda^2 U$ close to the limit of stability of the homogeneous phase, a dominant roton minimum is developed at the wave vector corresponding to the main minimum of the pair interaction potential ($k = 1$), signaling an instability towards the formation of modulated patterns with this characteristic wave vector. We found that the limit of Bogoliubov stability of the homogeneous phase is rather close to the actual boundary of the superfluid and homogeneous phases.

We studied simultaneously the superfluid fraction f_s, estimated using a well-established adaptation of Leggett's criterion [55,65], and the density contrast C. Our results suggest that, close to the superfluid phase boundary (see Fig. 6), the QCP hosts a supersolid state in which quasicrystalline order and superfluidity simultaneously emerge [33]. The combination of a many-mode variational minimization and an accurate calculation of the Leggett's superfluid fraction allowed us to distinguish also the phase boundary of this supersolidlike QCP.

Finally, we notice that, although we focused on a selected class of interactions, the methodology applied here is general and can be used with other types of potentials. Our results provide a solid basis for the search for physical systems where tunable two-body interactions are capable of stabilizing many-body quantum quasicrystal phases of the kind described in this paper.

ACKNOWLEDGMENTS

A.M.-C. acknowledges financial support from Fundação de Amparo à Pesquisa de Santa Catarina, Brazil (Fapesc). A.M.-C. acknowledges R. Cenci for helpful discussions. R.T. thanks the Physics Department of the Universidade Federal de Santa Catarina for full support. This study was financed in part by the Coordenação de Aperfeiçoamento de Pessoal de Nível Superior - Brasil (CAPES), Finance Code 001. T.M. acknowledges CNPq for support through Bolsa de produtividade em Pesquisa No. 311079/2015-6. T.M. and V.Z. are supported by the Serrapilheira Institute (Grant No. Serra-1812-27802). The numerical integration of the Gross-Pitaevskii equation was done with the help of the software XMDS2 [66].

[1] L. Zhou, *Introduction to Soft Matter Physics* (World Scientific, Singapore, 2019).
[2] R. Zhang, A. Mozaffari, and J. J. de Pablo, Nat. Rev. Mater. **6**, 437 (2021).
[3] K. A. Müller, *Stripes and Related Phenomena*, edited by A. Bianconi and N. L. Saini (Springer, Boston, 2000), pp. 1–8.
[4] M. Fratini, N. Poccia, A. Ricci, G. Campi, M. Burghammer, G. Aeppli, and A. Bianconi, Nature (London) **466**, 841 (2010).
[5] A. Aumann, T. Ackemann, E. Große Westhoff, and W. Lange, Phys. Rev. E **66**, 046220 (2002).
[6] R. Herrero, E. Große Westhoff, A. Aumann, T. Ackemann, Y. A. Logvin, and W. Lange, Phys. Rev. Lett. **82**, 4627 (1999).

[7] E. Pampaloni, P. L. Ramazza, S. Residori, and F. T. Arecchi, Phys. Rev. Lett. **74**, 258 (1995).

[8] F. Böttcher, J.-N. Schmidt, J. Hertkorn, K. S. H. Ng, S. D. Graham, M. Guo, T. Langen, and T. Pfau, Rep. Prog. Phys. **84**, 012403 (2021).

[9] L. Chomaz, S. Baier, D. Petter, M. J. Mark, F. Wächtler, L. Santos, and F. Ferlaino, Phys. Rev. X **6**, 041039 (2016).

[10] L. Tanzi, J. G. Maloberti, G. Biagioni, A. Fioretti, C. Gabbanini, and G. Modugno, Science **371**, 1162 (2021).

[11] F. Cinti and M. Boninsegni, Phys. Rev. A **96**, 013627 (2017).

[12] F. Cinti, A. Cappellaro, L. Salasnich, and T. Macrì, Phys. Rev. Lett. **119**, 215302 (2017).

[13] K. Deguchi, S. Matsukawa, N. K. Sato, T. Hattori, K. Ishida, H. Takakura, and T. Ishimasa, Nat. Mater. **11**, 1013 (2012).

[14] N. K. Sato, S. Matsukawa, K. Nobe, K. Imura, K. Deguchi, and T. Ishimasa, J. Phys. Conf. Ser. **868**, 012005 (2017).

[15] N. Defenu, T. Donner, T. Macrì, G. Pagano, S. Ruffo, and A. Trombettoni, arXiv:2109.01063 [cond-mat.quant-gas].

[16] G. Campos-Villalobos, M. Dijkstra, and A. Patti, Phys. Rev. Lett. **126**, 158001 (2021).

[17] T. Dotera, Isr. J. Chem. **51**, 1197 (2011).

[18] G. Malescio and G. Pellicane, Phys. Rev. E **70**, 021202 (2004).

[19] A. Kumar and V. Molinero, J. Phys. Chem. Lett. **8**, 5053 (2017).

[20] K. Barkan, H. Diamant, and R. Lifshitz, Phys. Rev. B **83**, 172201 (2011).

[21] K. Barkan, M. Engel, and R. Lifshitz, Phys. Rev. Lett. **113**, 098304 (2014).

[22] C. N. Likos, Phys. Rep. **348**, 267 (2001).

[23] T. Dotera, T. Oshiro, and P. Ziherl, Nature (London) **506**, 208 (2014).

[24] K. Viebahn, M. Sbroscia, E. Carter, J.-C. Yu, and U. Schneider, Phys. Rev. Lett. **122**, 110404 (2019).

[25] M. Sbroscia, K. Viebahn, E. Carter, J.-C. Yu, A. Gaunt, and U. Schneider, Phys. Rev. Lett. **125**, 200604 (2020).

[26] R. Gautier, H. Yao, and L. Sanchez-Palencia, Phys. Rev. Lett. **126**, 110401 (2021).

[27] M. Ciardi, T. Macrì, and F. Cinti, Phys. Rev. A **105**, L011301 (2022).

[28] F. Cinti, P. Jain, M. Boninsegni, A. Micheli, P. Zoller, and G. Pupillo, Phys. Rev. Lett. **105**, 135301 (2010).

[29] F. Cinti, T. Macrì, W. Lechner, G. Pupillo, and T. Pohl, Nat. Commun. **5**, 3235 (2014).

[30] B. R. de Abreu, F. Cinti, and T. Macrì, Phys. Rev. B **105**, 094505 (2022).

[31] J. Hou, H. Hu, K. Sun, and C. Zhang, Phys. Rev. Lett. **120**, 060407 (2018).

[32] F. Mivehvar, H. Ritsch, and F. Piazza, Phys. Rev. Lett. **123**, 210604 (2019).

[33] G. Pupillo, P. Ziherl, and F. Cinti, Phys. Rev. B **101**, 134522 (2020).

[34] F. Cinti, Phys. Rev. B **100**, 214515 (2019).

[35] V. D. Vaidya, Y. Guo, R. M. Kroeze, K. E. Ballantine, A. J. Kollár, J. Keeling, and B. L. Lev, Phys. Rev. X **8**, 011002 (2018).

[36] S. Gopalakrishnan, B. L. Lev, and P. M. Goldbart, Nat. Phys. **5**, 845 (2009).

[37] S. Gopalakrishnan, B. L. Lev, and P. M. Goldbart, Phys. Rev. A **82**, 043612 (2010).

[38] Y.-C. Zhang, V. Walther, and T. Pohl, Phys. Rev. A **103**, 023308 (2021).

[39] S. Prestipino, A. Sergi, and E. Bruno, Phys. Rev. B **98**, 104104 (2018).

[40] S. Prestipino, A. Sergi, and E. Bruno, J. Phys. A: Math. Theor. **52**, 015002 (2019).

[41] V. Heinonen, K. J. Burns, and J. Dunkel, Phys. Rev. A **99**, 063621 (2019).

[42] S. K. Mkhonta, K. R. Elder, and Z.-F. Huang, Phys. Rev. Lett. **111**, 035501 (2013).

[43] C. N. Likos, A. Lang, M. Watzlawek, and H. Löwen, Phys. Rev. E **63**, 031206 (2001).

[44] C. N. Likos, B. M. Mladek, A. J. Moreno, D. Gottwald, and G. Kahl, Comput. Phys. Commun. **179**, 71 (2008).

[45] M. A. Glaser, G. M. Grason, R. D. Kamien, A. Košmrlj, C. D. Santangelo, and P. Ziherl, Europhys. Lett. **78**, 46004 (2007).

[46] A. Mendoza-Coto, D. d. S. Caetano, and R. Díaz-Méndez, Phys. Rev. A **104**, 013301 (2021).

[47] A. Mendoza-Coto, R. Cenci, G. Pupillo, R. Díaz-Méndez, and E. Babaev, Soft Matter **17**, 915 (2021).

[48] J. Toner and D. R. Nelson, Phys. Rev. B **23**, 316 (1981).

[49] D. G. Barci and D. A. Stariolo, Phys. Rev. Lett. **98**, 200604 (2007).

[50] T. Macrì, F. Maucher, F. Cinti, and T. Pohl, Phys. Rev. A **87**, 061602(R) (2013).

[51] S. Prestipino and F. Saija, J. Chem. Phys. **141**, 184502 (2014).

[52] P. Kroiss, M. Boninsegni, and L. Pollet, Phys. Rev. B **93**, 174520 (2016).

[53] M. Boninsegni and N. V. Prokof'ev, Rev. Mod. Phys. **84**, 759 (2012).

[54] G. V. Chester, Phys. Rev. A **2**, 256 (1970).

[55] A. J. Leggett, Phys. Rev. Lett. **25**, 1543 (1970).

[56] N. Henkel, R. Nath, and T. Pohl, Phys. Rev. Lett. **104**, 195302 (2010).

[57] Y. Li, G. I. Martone, L. P. Pitaevskii, and S. Stringari, Phys. Rev. Lett. **110**, 235302 (2013).

[58] R. Liao, Phys. Rev. Lett. **120**, 140403 (2018).

[59] G. Natale, R. M. W. van Bijnen, A. Patscheider, D. Petter, M. J. Mark, L. Chomaz, and F. Ferlaino, Phys. Rev. Lett. **123**, 050402 (2019).

[60] L. Tanzi, S. M. Roccuzzo, E. Lucioni, F. Famà, A. Fioretti, C. Gabbanini, G. Modugno, A. Recati, and S. Stringari, Nature (London) **574**, 382 (2019).

[61] L. Tanzi, E. Lucioni, F. Famà, J. Catani, A. Fioretti, C. Gabbanini, R. N. Bisset, L. Santos, and G. Modugno, Phys. Rev. Lett. **122**, 130405 (2019).

[62] F. Böttcher, J.-N. Schmidt, M. Wenzel, J. Hertkorn, M. Guo, T. Langen, and T. Pfau, Phys. Rev. X **9**, 011051 (2019).

[63] L. Chomaz, D. Petter, P. Ilzhöfer, G. Natale, A. Trautmann, C. Politi, G. Durastante, R. M. W. van Bijnen, A. Patscheider, M. Sohmen, M. J. Mark, and F. Ferlaino, Phys. Rev. X **9**, 021012 (2019).

[64] M. A. Norcia, C. Politi, L. Klaus, E. Poli, M. Sohmen, M. J. Mark, R. N. Bisset, L. Santos, and F. Ferlaino, Nature (London) **596**, 357 (2021).

[65] Y.-C. Zhang, F. Maucher, and T. Pohl, Phys. Rev. Lett. **123**, 015301 (2019).

[66] G. R. Dennis, J. J. Hope, and M. T. Johnsson, Comput. Phys. Commun. **184**, 201 (2013).

[67] F. Ancilotto, M. Rossi, and F. Toigo, Phys. Rev. A **88**, 033618 (2013).

[68] L. Pitaevskii and S. Stringari, *Bose-Einstein Condensation*, International Series of Monographs on Physics (Clarendon, Oxford, 2003), p. 492.

[69] C. J. Pethick and H. Smith, *Bose-Einstein Condensation in Dilute Gases* (Cambridge University Press, Cambridge, 2008), p. 584.